Acoustic Wave Heating of the Thermosphere

Michael P. Hickey Ph.D.
Embry-Riddle Aeronautical University, hicke0b5@erau.edu

G. Schubert
Institute of Geophysics and Planetary Physics, University of California

R. L. Walterscheid
The Aerospace Corporation

Acoustic wave heating of the thermosphere

M. P. Hickey

Department of Physics and Astronomy, Clemson University, Clemson, South Carolina, USA

G. Schubert

Space Science Applications Laboratory, The Aerospace Corporation, Los Angeles, California, USA

Department of Earth and Space Sciences, Institute of Geophysics and Planetary Physics, University of California, Los Angeles, California, USA

R. L. Walterscheid

Space Science Applications Laboratory, The Aerospace Corporation, Los Angeles, California, USA

Abstract. A numerical model is used to study the dissipation in the thermosphere of upward propagating acoustic waves. Whereas dissipating gravity waves can cool the upper atmosphere through the effects of sensible heat flux divergence, it is found that acoustic waves mainly heat the thermosphere by viscous dissipation. Though the amplitudes of acoustic waves in the atmosphere are poorly constrained, the calculations suggest that dissipating acoustic waves can locally heat the thermosphere at rates of tens of kelvins per day and thereby contribute to the thermospheric energy balance. It is shown that viscous heating cannot be calculated from the divergence of the wave mechanical energy flux. Acoustic waves that are barely detectable at mesopause heights can become significant heaters of the atmosphere high in the thermosphere. We suggest that acoustic waves might be responsible for heating the equatorial F region to produce the hot spot observed in the O I 630 nm airglow over the Andes Mountains.

1. Introduction

It has long been appreciated that the dissipation of upward propagating internal gravity waves could provide a net cooling of the upper atmosphere through the dynamical effects of sensible heat flux divergence and their predominance over viscous heating [*Walterscheid*, 1981]. However, the competition between cooling by sensible heat flux divergence and heating by viscous dissipation has not heretofore been investigated for the dissipation of upward propagating acoustic waves. Perhaps this is because the role of acoustic waves in the thermal balance of the upper atmosphere is still largely unknown. However, there is evidence that acoustic waves, generated in the lower atmosphere by, for example, strong thunderstorms and ocean waves, propagate into the thermosphere [*Rind*, 1977, 1978; *Raju et al.*, 1981; *Hecht et al.*, 1995]. It is therefore prudent to investigate the possible influence of acoustic waves on the thermal state of the upper atmosphere; we do this in the present paper with a particular focus on the question of whether the dissipation of acoustic waves cools the thermosphere by sensible heat flux divergence or heats it by viscous dissipation.

2. Model

The upward propagation of acoustic waves is calculated with a full-wave model that solves the complete linearized equations of continuity, momentum, and energy for a compressible, viscous, and thermally conducting atmosphere with arbitrary altitude variations in basic state thermal structure. Unlike WKB models, the full-wave model rigorously accounts for wave reflection. Details of

the model can be found in the work of *Hickey et al.* [2000]. The model domain extends from the surface to an altitude of 500 km. A sponge layer at the top of the model domain insures against spurious wave reflections from the upper boundary. Waves are forced at a height of 20 km by specifying the amplitude of the temperature perturbation. Wave amplitudes are scaled to give a wave mechanical energy flux of 1.25×10^{-5} W m^{-2} at an altitude of 30 km. This value is based on the requirement that the maximum perturbation horizontal velocity of the waves be $\sim$38 m s^{-1} at F-region altitudes, a value suggested from the radar observations of *Raju et al.* [1981].

2.1. Model Parameters

Figure 1 (top) shows altitude profiles of the basic state sound speed and the acoustic cutoff period. We will consider the upward propagation of fast acoustic waves with periods and horizontal wavelengths of 10 s and 6 km, 2 min and 72 km, and 4 min and 144 km. The three waves have horizontal phase velocities of 600 m s^{-1}. According to Figure 1 (top) the horizontal propagation of the waves is supersonic at altitudes less than about 168 km and subsonic at greater heights. The periods of the three waves that we consider are smaller than the acoustic cutoff period at all heights except for the 4 min wave period which exceeds the acoustic cutoff period in the approximate altitude interval 100–117 km. The waves have periods that span the low-frequency domain of acoustic wave periods. Intercomparison of the waves is facilitated by having the same horizontal phase velocity for all the waves. As a consequence, the waves have horizontal wavelengths varying by more than an order of magnitude.

The altitude profiles of momentum and thermal diffusivities are shown in Figure 1 (bottom). The molecular coefficients of viscosity μ_m and thermal conductivity k_m are taken from *Rees* [1989] and are used to calculate the molecular momentum diffusivity $\eta_m = \mu_m/\rho$ and molecular thermal diffusivity $k_m/\rho c_p$, where ρ is the atmospheric density and c_p is the specific heat at constant pressure.
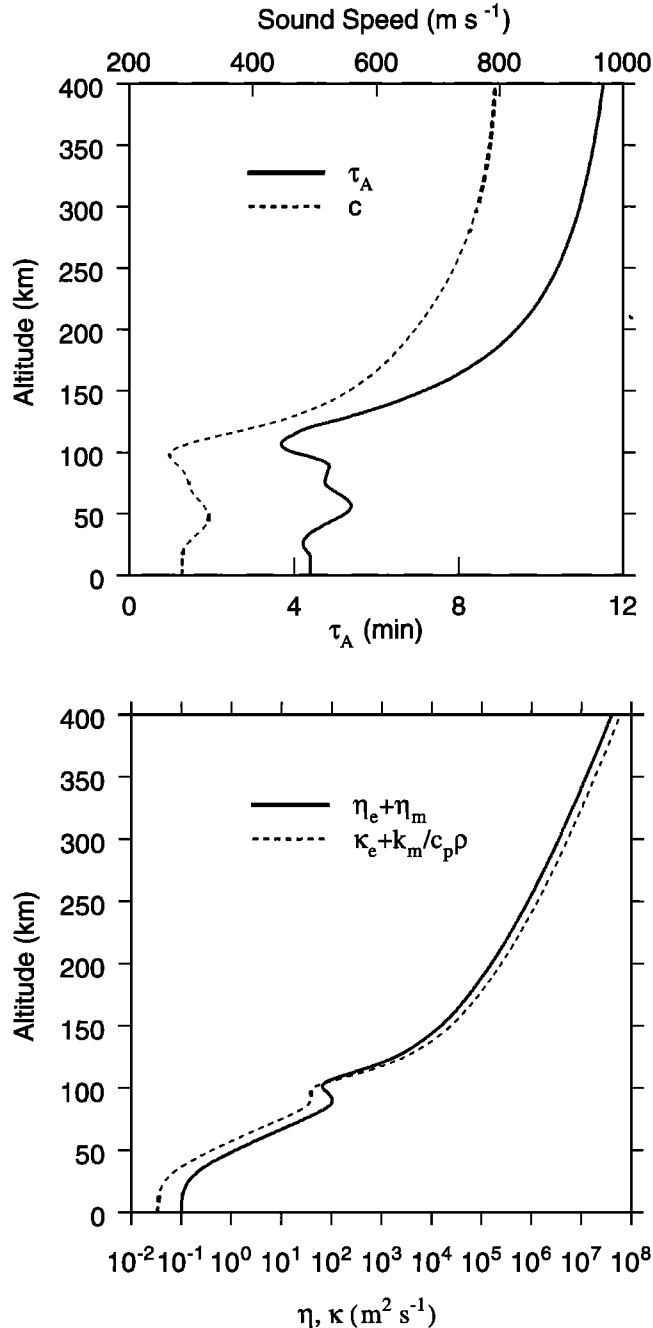
Figure 1. (top) Altitude profiles of sound speed (c, dashed curve) and acoustic cutoff period (τ_A, solid curve) for the basic state. (bottom) Altitude profiles of momentum η and thermal κ diffusivities. Subscript e denotes eddy values and subscript m refers to molecular values; k is thermal conductivity, ρ is density, and c_p is specific heat at constant pressure.

The eddy momentum diffusivity η_e approximates that given by *Strobel* [1989] and has a maximum value of 100 m^2 s^{-1} at a 90 km altitude. The eddy thermal diffusivity κ_e is calculated from the eddy momentum diffusivity by assuming a Prandtl number of 3 [*Strobel*, 1989]. Between the ground and the 90 km altitude both momentum and thermal diffusivities are dominated by the eddy contributions, which cause the diffusivities to increase with height. Above the mesopause the diffusivities are dominated by the molecular contributions, which cause the diffusivities to increase with height in the thermosphere.

2.2. Wave Heating and Cooling

Hickey et al. [2000] show that to second order, waves heat or cool the background atmosphere at the rate Q (degrees per unit time) given by

$$\rho c_p Q = -\langle \underline{\sigma}'_m : \underline{\nabla}\,\underline{u}' \rangle - \frac{d}{dz}\left\{ \frac{\overline{\rho} c_p \overline{T}}{\overline{\theta}} \langle w'\theta' \rangle \right\} - \frac{\overline{\rho} g}{\overline{\theta}} \langle w'\theta' \rangle - \frac{1}{\overline{\rho} c_p \overline{T}}$$

$$\times \langle p'\underline{\nabla}(k_m \underline{\nabla} T') \rangle - \frac{1}{\overline{\rho}\overline{\theta}} \langle p'\underline{\nabla}(\overline{\rho}\kappa_e \underline{\nabla}\theta') \rangle. \qquad (1)$$

In (1) the angle brackets denote an x, y, t average (x and y are horizontal Cartesian coordinates, t is time), z is altitude, T is temperature, u' is the wave velocity vector, θ is potential temperature, $\underline{\sigma}'_m$ is the molecular viscous stress tensor of the wave field, w' is the wave vertical velocity, p' is the wave pressure perturbation, g is the acceleration of gravity, primes refer to wave quantities, and overbars refer to basic state quantities. In (1) the first term on the right-hand side is the heating rate due to viscous dissipation of wave kinetic energy (designated Q_{vis}). We will compare the viscous dissipation heating rate with the negative divergence of the wave mechanical energy flux $-\frac{d}{dz}\langle w'p' \rangle$, a quantity often used to estimate the viscous heating. However, there are other channels for the wave energy flux which do not produce local heating [*Hickey et al.*, 2000]. The second term on the right-hand side of (1) is closely related to the sensible heat flux divergence $-\frac{d}{dz}\langle w'\theta' \rangle$. The third term on the right-hand side of (1) represents the change in gravitational potential by the vertical transport of heat. The sum of the last two terms on the right-hand side of (1) is designated $Q_{p'D'}$: it represents a second-order diffusion of heat and always produces net heating in our simulations.

3. Results

Figure 2 shows altitude profiles of the amplitude and phase of the temperature perturbation of the three acoustic waves. The phase of the 10 s wave (dashed curve) indicates that it is vertically propagating at all altitudes. The temperature amplitude of the 10 s wave (solid curve) increases with height from the surface to about a 140 km altitude where it reaches a maximum. Molecular viscosity and thermal conduction mainly damp the 10 s wave at higher altitudes. The dominant role of molecular viscosity and thermal conduction in damping the 10 s wave at altitudes above about 140 km is confirmed by an adiabatic calculation (not shown here) which shows that the 10 s wave becomes evanescent only at altitudes greater than about 160 km when viscosity and thermal conduction have almost entirely damped the wave. The phase propagation with large vertical wavelength and negligible amplitude at altitudes above about 160 km is due to effects of molecular viscosity and thermal conduction. Below 100 km altitude the vertical wavelength is ∼3.4 km, and it increases to ∼10 km near 150 km altitude. The maximum amplitude of the wave horizontal velocity perturbation (not shown) is 2.74 m s^{-1}.

The altitude profile of the phase of the 2 min wave in Figure 2 (dashed curve) indicates standing wave behavior due to reflections below a height of about 125 km and vertical propagation at higher altitudes. The amplitude of the temperature perturbation of the 2 min wave (solid curve) peaks at an altitude of about 170 km. The decrease in wave amplitude with height above this altitude is mainly the result of evanescence and not viscous damping as confirmed by adiabatic calculations not shown here. In fact, the adiabatic calculations show that the 2 min wave is evanescent above 125 km altitude and grows in amplitude between 125 and 170 km due to weak evanescence and the decrease in density with height. The phase propagation at altitudes above about 125 km is due to effects of molecular viscosity and thermal conduction. There is a secondary local maximum in the temperature perturbation amplitude of the 2 min wave at a height of about 120 km, just
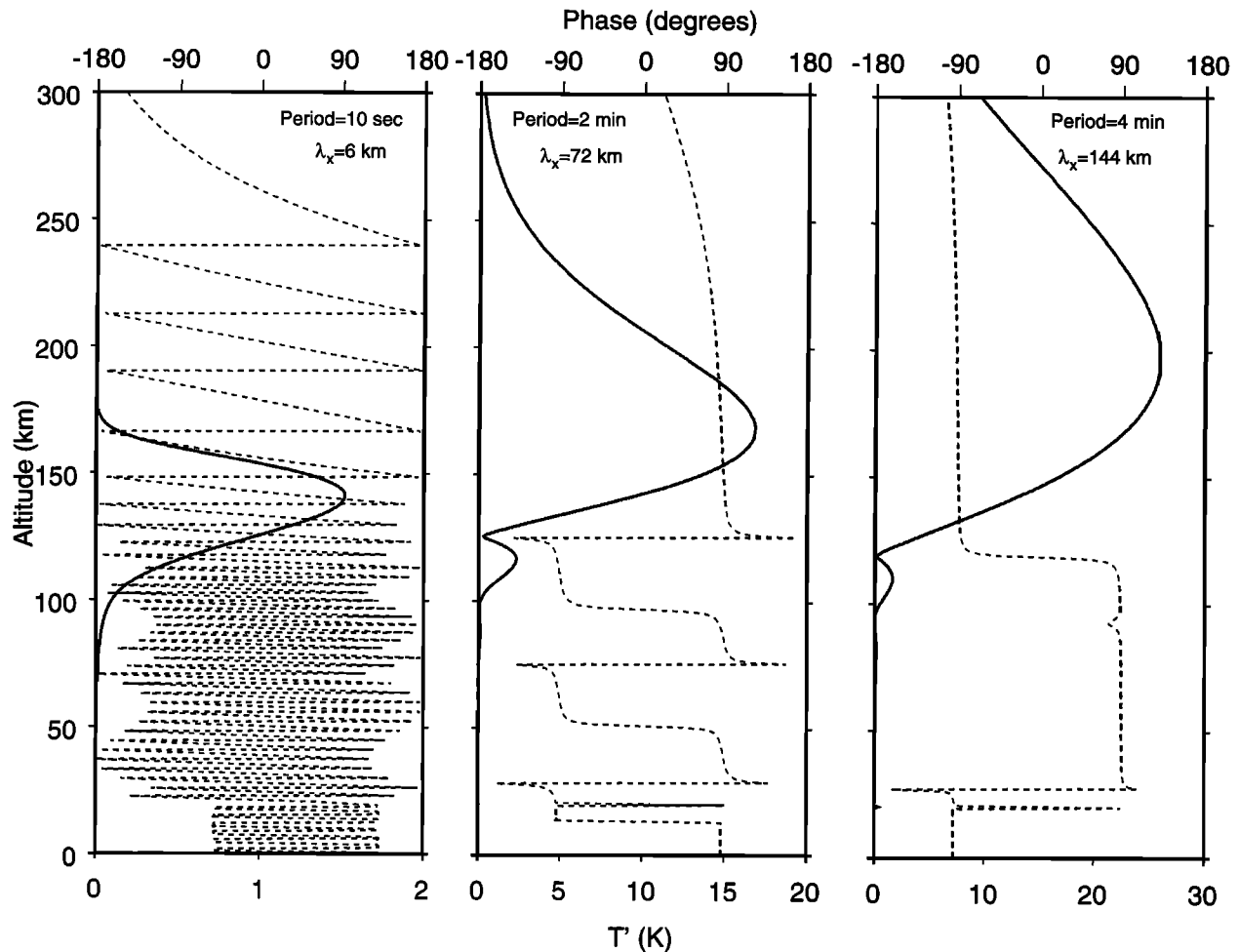
Figure 2. Amplitude (denoted by T' and given by the solid curve) and phase (dashed curve) of three acoustic waves as a function of height.

below the altitude of reflection at about 125 km. The maximum amplitude of the wave horizontal velocity perturbation (not shown) is 28.4 m s^{-1}.

The altitude profile of the phase of the temperature perturbation of the 4 min wave (dashed curve) indicates partial reflection at heights less than about 125 km and vertical propagation at higher altitudes. The temperature perturbation of the 4 min wave (solid curve) reaches a maximum amplitude at a height of about 195 km; the decrease in temperature perturbation amplitude with height at higher altitudes is mainly due to evanescence, as shown by adiabatic calculations not reported here. As was the case with the 2 min wave, the growth in temperature perturbation amplitude of the 4 min wave between altitudes of about 125 and 195 km is due to weak evanescent behavior. The phase propagation at altitudes above about 125 km is due to effects of molecular viscosity and thermal conduction. A secondary local maximum in the temperature perturbation amplitude of the 4 min wave occurs at a height of about 120 km, similar to the secondary temperature amplitude maximum of the 2 min wave. The maximum amplitude of the wave horizontal velocity perturbation (not shown) is 38.0 m s^{-1}.

Figure 3 shows altitude profiles of the viscous heating rate (dashed-dotted curve), the sensible heat flux divergence term given in (1) (short-dashed curve), the sum of the last two terms in (1) (designated as $Q_{p'D'}$ and represented by the long-dashed curve), and the sum of all terms (solid curve) for the three acoustic waves. For the 10 s wave the viscous heating maximizes near 140 km altitude, while the sensible heat flux divergence is negligible at all

heights. The total heating rate, which for this wave is essentially given by the sum of Q_{vis} and $Q_{p'D'}$, achieves a maximum value of ~11 K d^{-1} near the 140 km altitude.

For the 2 min wave the viscous heating rate in Figure 3 maximizes near 210 km altitude, while the sensible heat flux divergence leads to small heating below about 175 km altitude and cooling at higher altitudes. The maximum total heating rate of ~43 K d^{-1} occurs near 200 km altitude.

For the 4 min wave the viscous heating rate maximizes near 300 km altitude. The divergence of the sensible heat flux cools the atmosphere above ~200 km altitude and slightly warms the atmosphere at lower altitudes. The maximum total heating rate of ~170 K d^{-1} occurs near 280 km altitude.

Figure 4 compares altitude profiles of the viscous heating rate and the negative divergence of the wave mechanical energy flux for the three acoustic waves. The latter has been widely used as an estimate of the former in acoustic-gravity wave studies [e.g., Hines, 1965; Rind, 1977; Young et al., 1997; Matcheva and Strobel, 1999]. For the 10 s wave the negative divergence of the wave mechanical energy flux overestimates the viscous heating rate by ~50%, although both profiles have a similar shape and maximize at approximately the same altitude. For the 2 min wave the maximum viscous heating rate of ~30 K d^{-1} occurs near the 210 km altitude, while the maximum value of the negative divergence of the wave mechanical energy flux of ~40 K d^{-1} occurs near the 195 km altitude. For the 4 min wave the divergence of the wave mechanical energy flux and viscous heating rate profiles have similar shapes and similar maximum values (~170
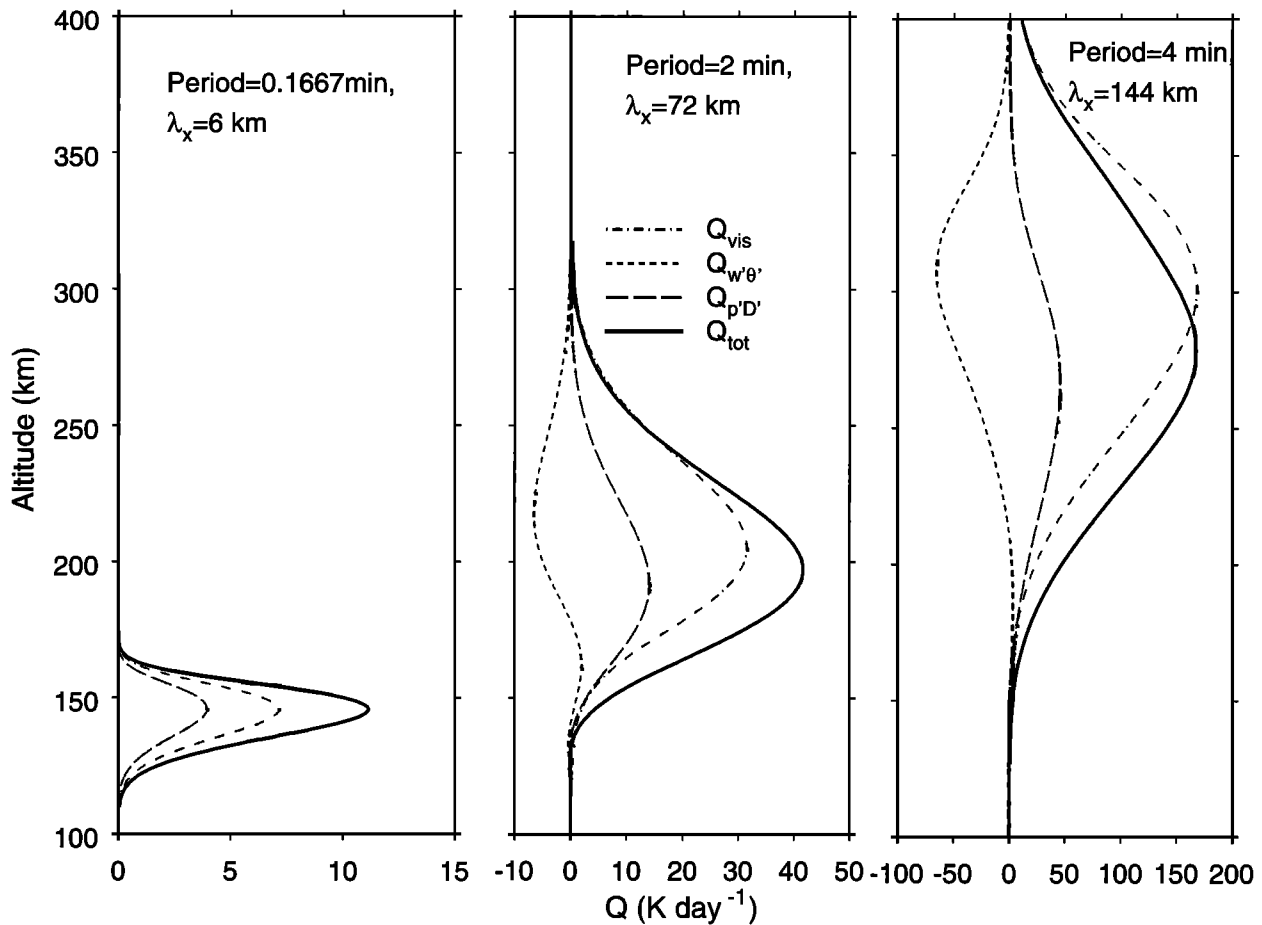
Figure 3. Altitude profiles of total wave heating/cooling (Q_{tot}, solid curve) wave heating by viscous dissipation (Q_{vis}, dashed-dotted curve), wave heating/cooling by the sensible heat flux divergence ($Q_{w'\theta'}$, short-dashed curve), and wave heating associated with the diffusion of heat ($Q_{p'D'}$, long-dashed curve) for the three waves of Figure 2. The quantity $Q_{w'\theta'}$ for the 10 s wave (left panel), is essentially zero.

K d^{-1}), but the maximum viscous heating rate occurs about 30 km higher than the former. It is clear from these results that the negative divergence of the wave mechanical energy flux does not provide a reliable estimate of viscous heating by wave dissipation.

4. Discussion and Conclusion

On the basis of the analysis of thunderstorm-generated acoustic waves as revealed in HF radar F-region phase height measurements, *Raju et al.* [1981] estimated that their observations could be attributed to acoustic waves having neutral perturbation horizontal velocities (u') of ~38 m s^{-1}. They further estimated that the flux of wave mechanical energy at F-region altitudes was ~5 × 10^{-5} W m^{-2}. We scaled the wave amplitudes such that the maximum value of u' was ~38 m s^{-1} for the 4 min wave, which corresponds to a wave mechanical energy flux of 1.25 × 10^{-5} W m^{-2} at 30 km altitude. This same value of energy flux at the 30 km altitude was also used for the 10 s and 2 min waves, for which the corresponding maximum values of u' were significantly less than 38 m s^{-1}, as given above. For the 4 min wave the wave mechanical energy flux (not shown) remains approximately constant in the lower thermosphere and then decreases slowly with increasing altitude after that, becoming 1.25 × 10^{-6} W m^{-2} at ~280 km altitude. This value is significantly smaller (by a factor of 40) than the estimate of

Raju et al. [1981]. The difference may be due to the fact that they estimated the energy flux, whereas we have used a numerical model to calculate it. Additionally, we have used a horizontal wavelength of 144 km for this wave, whereas their observations provided no information on this value.

In a study of the dissipation of observed acoustic waves with 5 s periods, *Rind* [1977] estimated that the vertical energy fluxes are ~5 × 10^{-5} W m^{-2} in the lower atmosphere. The source of these waves is large wintertime ocean waves in the Atlantic Ocean off the coast of Palisades. He demonstrated that these waves would most likely dissipate in the lower thermosphere between altitudes of about 110 and 140 km and could produce heating rates as large as 30 K d^{-1}. This value of energy flux is the same as we used here, as described in the previous paragraph. The maximum heating rate derived for our 10 s wave using this value of energy flux is about 11 K d^{-1} at the 140 km altitude. This compares favorably with *Rind*'s [1977] estimate of 30 K d^{-1}, although the wave periods in the two cases are not identical, and *Rind* [1977] did not discuss the horizontal wavelengths of the observed waves.

Although we have found that the instantaneous heating rates in the thermosphere due to the viscous dissipation of upward propagating acoustic waves can be large, this heating would typically occur over a limited spatial domain and for a limited time. If wave sources in the troposphere are spatially localized, then geometric spreading will occur as the waves propagate upward, reducing wave amplitudes compared to our calculated values and also reducing instantaneous heating rates. Therefore the combined
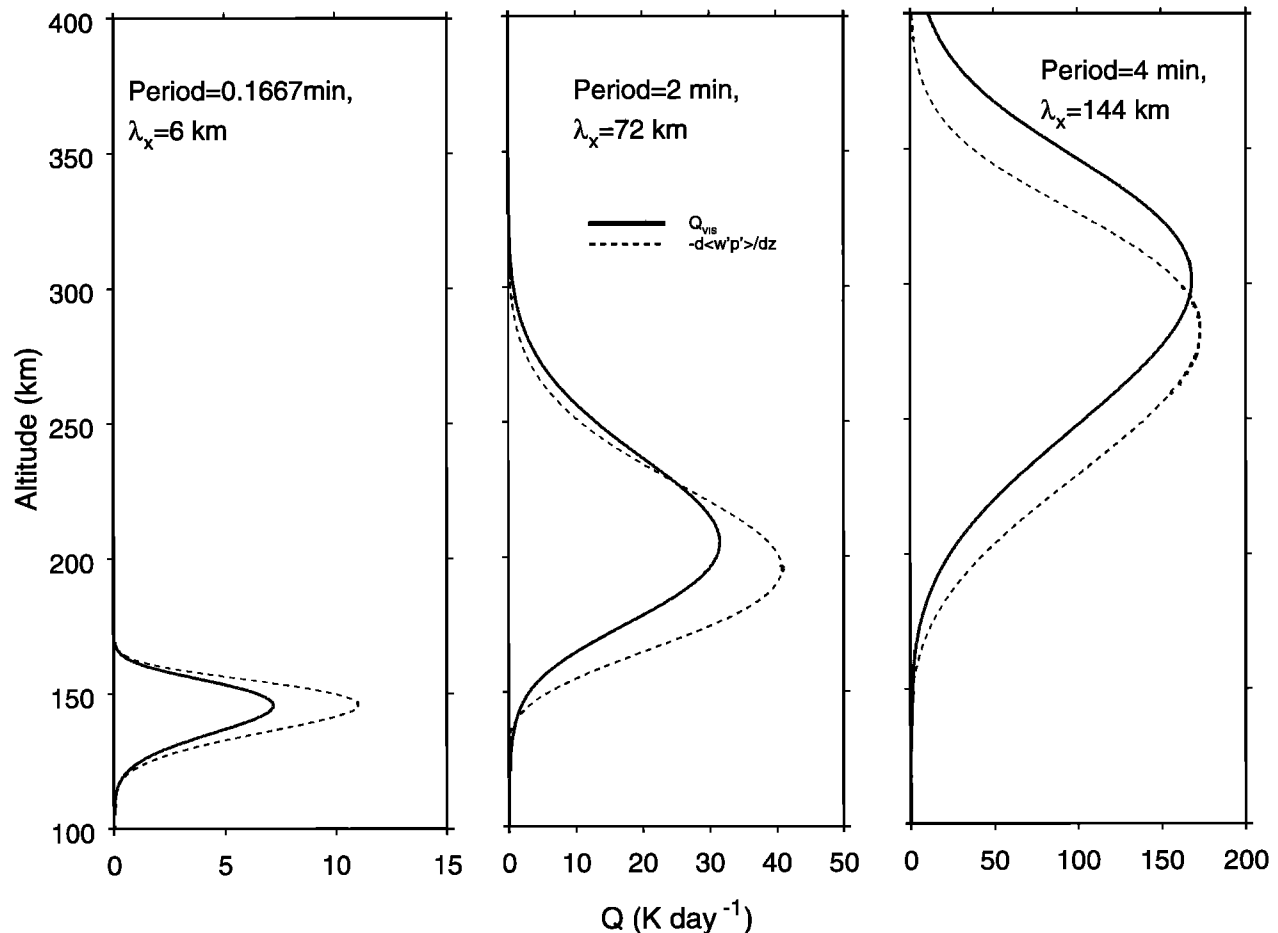
Figure 4. A comparison, over altitude, of wave heating by viscous dissipation with the divergence of the wave mechanical energy flux for the three waves of Figure 2. The divergence of the wave mechanical energy flux does not provide a good estimate of the wave viscous heating.

effects of geometric spreading and intermittent and spatially localized wave sources will reduce the acoustic wave heating calculated here. Nonetheless, the heating rates are significant and should perhaps be incorporated into thermal and dynamical models of the thermosphere.

We have shown that the viscous heating rate cannot be approximated by the divergence of the wave mechanical energy flux. The viscous heating rate is smaller than the divergence of the wave mechanical energy flux, and the two often maximize at different altitudes. Similar results were found for large-scale gravity waves dissipating in the atmosphere of Jupiter, where the divergence of the wave mechanical energy flux overestimated the viscous heating rate by a factor of about 2 [*Hickey et al.*, 2000].

The scaling we adopted for the acoustic wave mechanical energy flux gives wave temperature amplitudes at mesopause heights that are several tenths of a degree (Figure 2). Mesopause airglow observations of sufficient temporal resolution and sensitivity should be able to detect these acoustic waves. Though the acoustic wave amplitudes are relatively small at an altitude of about 100 km, the wave amplitudes 50–100 km higher in the thermosphere are several to tens of kelvins. Moreover, these waves give heating rates of tens to a hundred kelvins per day when they dissipate at heights of 150–300 km in the thermosphere. Acoustic waves that are barely detectable at mesopause heights can become prodigious heaters of the atmosphere high in the thermosphere.

The equatorial F-region hot spot observed by *Meriwether et al.* [1996, 1997] in the O I 630 nm airglow over the Andes Mountains may be a consequence of acoustic wave heating of the thermo-

sphere. Wave heating of this region of the atmosphere is suggested by the observations of enhanced temperature variability [*Meriwether et al.*, 1996, 1997]. Most gravity waves do not penetrate to high thermospheric altitudes [*Taylor et al.*, 1993; *Swenson et al.*, 1995]. *Meriwether et al.* [1997] suggest that gravity waves with vertical wavelengths larger than about 40–50 km might get high enough to produce the hot spot; we suggest that acoustic waves, which more readily reach F-region altitudes, might instead be responsible for the heating.

References

Hecht, J. H., S. K. Ramsay Howat, R. L. Walterscheid, and J. R. Isler, Observations of spectra of intensity fluctuations of the OH Meinel nightglow during ALOHA-93, *Geophys. Res. Lett.*, *22*, 2873–2876, 1995.

Hickey, M. P., R. L. Walterscheid, and G. Schubert, Gravity wave heating and cooling in Jupiter's thermosphere, *Icarus*, *148*, 266–281, 2000.

Hines, C. O., Dynamical heating of the upper atmosphere, *J. Geophys. Res*, *70*, 177– 183, 1965.

Matcheva, K. I., and D. F. Strobel, Heating of Jupiter's thermosphere by dissipation of gravity waves due to molecular viscosity and heat conduction, *Icarus*, *140*, 328–340, 1999.

Meriwether, J. W., J. L. Mirick, M. A. Biondi, F. A. Herrero, and C. G. Fesen, Evidence for orographic wave heating in the equatorial thermosphere at solar maximum, *Geophys. Res. Lett.*, *23*, 2177–2180, 1996.

Meriwether, J. W., M. A. Biondi, F. A. Herraro, C. G. Fesen, and D. C. Hallenback, Optical interferometric studies of the nighttime equatorial thermosphere: Enhanced temperatures and zonal wind gradients, *J. Geophys. Res.*, *102*, 20,041–20,058, 1997.

Raju, D. G. K., M. S. Rao, B. M. Rao, C. Jogulu, C. P. Rao, and R. Ramanadham, Infrasonic oscillations in the F_2 region associated with severe thunderstorms, *J. Geophys. Res.*, *86*, 5873–5880, 1981.

Rees, M. H. ; *Physics and Chemistry of the Upper Atmosphere*, Cambridge Univ. Press, New York, 1989.

Rind, D., Heating of the lower thermosphere by the dissipation of acoustic waves, *J. Atmos. Sol. Terr. Phys.*, *39*, 445–456, 1977.

Rind, D., Investigation of the lower thermosphere results of ten years of continuous observations with natural infrasound, *J. Atmos. Sol. Terr. Phys.*, *40*, 1199–1210, 1978.

Strobel, D. F., Constraints on gravity wave induced diffusion in the middle atmosphere, *Pure Appl. Geophys.*, *130*, 533–546, 1989.

Swenson, G. R., C. S. Gardner, and M. J. Taylor, Maximum altitude penetration of atmospheric gravity waves observed during ALOHA-93, *Geophys. Res. Lett.*, *22*, 2857–2860, 1995.

Taylor, M. J., E. H. Ryan, T. F. Tuan, and R. Edwards, Evidence of preferred directions for gravity wave propagation due to wind filtering in the middle atmosphere, *J. Geophys. Res.*, *98*, 6047–6058, 1993.

Walterscheid, R. L., Dynamical cooling induced by dissipating internal gravity waves, *Geophys. Res. Lett.*, *8*, 1235–1238, 1981.

Young, L. A., R. V. Yelle, R. Young, A. Seiff, and D. B. Kirk, Gravity waves in Jupiter's thermosphere, *Science*, *276*, 108–111, 1997.

M. P. Hickey, Department of Physics and Astronomy, Clemson University, 308 Kinard Laboratory, Clemson, SC 29634-0978, USA. (hickey@hubcap.clemson.edu)

G. Schubert, Department of Earth and Space Sciences, Institute of Geophysics and Planetary Physics, University of California, Los Angeles, CA 90095-1567, USA. (schubert@ucla.edu)

R. L. Walterscheid, Space Science Applications Laboratory, The Aerospace Corporation, Los Angeles, CA 90009, USA. (richard.walterscheid@aero.org)